

Dynamical theory of thermal neutron scattering. II. *Pendellösung* in inelastic peaks*

Sushil Kumar Mendiratta[†]

IBM System Products Division, East Fishkill, Hopewell Junction, New York 12533

(Received 23 September 1975)

A theory is presented in which the effect of the dynamical theory of diffraction on inelastic one-phonon peaks is taken into account to the first order in neutron-phonon interaction. In this theory, the distorted-wave Born approximation for the neutron-lattice Hamiltonian is used; the inelastic scattering amplitude for a phonon is then shown to be a coherent sum of the inelastic amplitudes due to all the plane-wave components of the Bloch waves that form the neutron wave function in the crystal under the stationary lattice condition. For this purpose, all the plane-wave components of the dynamical theory of the elastic scattering are on equal footing in determining the inelastic amplitude. The result is then a wavelength- and thickness-dependent structure in one-phonon peaks. An experimental configuration is suggested for observing *Pendellösung* effects in one-phonon peaks.

INTRODUCTION

Thermal neutrons, when used as probe particles, differ from the other probe-particle beams, such as x rays and electrons, in two important respects. One is that the spinor nature of the neutrons facilitates the determination of the magnetic structure of the target material. The other is that the relative ease and accuracy with which one can do the energy analysis of the scattered beam make it possible to measure one-phonon cross sections accurately and thus obtain excitation spectra of the lattice. In¹ paper I we discussed the elastic scattering (diffraction) of the spinor neutron from a general magnetic lattice. In the following we discuss the effect of the dynamical theory of diffraction on the coherent inelastic scattering of a neutron.

In the past, the effect of thermal vibrations on the scattering from a solid has been investigated from two different points of view. The investigators in one category²⁻⁵ have aimed at determining the effect of thermal vibrations on the elastic peaks from a static lattice. The important features of this approach have been rather nicely elucidated by Yoshioka,² who treated thermal vibrations as giving rise to an extra, complex periodic potential on top of the periodic potential of the static lattice. These complex potentials, then, modify the profile of the elastic Bragg peaks, besides introducing the Debye-Waller factor. All of these treatments neglect the correlation between the displacements of different atoms that are caused by thermal vibrations. From this point of view the contribution of thermal vibrations as detailed in these treatments can be described as an incoherent contribution to the Bragg peaks.

The papers in the second category⁶⁻⁹ deal with the problem of explicitly determining the profile

of the inelastic peak. The interest of diffraction theorists in this problem was stimulated by investigations of the plasmon peak in high-energy electron diffraction. This peak appears in the energy-loss spectrum of the transmitted primary beam. Two slightly different methods of treating this problem have been given by Howie⁷ and by Fujimoto and Kainuma.⁸ Both methods lead to the same physical result; that is, they give a structure in the energy-loss profile of an inelastic peaks, which is dependent on thickness or incident wavelength. When electrons are the probe particles, however, the structure is somewhat washed out because of integration over the energy window of the detector. Only with thermal neutrons can one obtain the precise energy-momentum resolution of a single phonon; there one can expect dramatic results.

In the following, we discuss the one-phonon coherent inelastic scattering of thermal neutrons from a nuclear lattice. We seek to determine the effect of dynamical diffraction on the inelastic peak, and in particular to explore the situation in which it might be possible to observe a *Pendellösung* phenomenon in the inelastic peak. We base our treatment on the ideas given by Fujimoto and Kainuma.⁸ Section I deals with the Hamiltonian of the neutron-lattice system and a suitable time-dependent wave function, which we use in computing the transition rates. In Sec. II we determine the intensity profile of an inelastic one-phonon peak. Section III deals with an inelastic *Pendellösung* effect, and Sec. IV is the final discussion of the results.

I. HAMILTONIAN OF THE SYSTEM AND TIME-DEPENDENT WAVE FUNCTION

We write the Hamiltonian of the neutron-lattice system as follows:

$$H = \frac{1}{2m} \left(\frac{\hbar}{i} \frac{\partial}{\partial \mathbf{x}} \right)^2 + \sum_{\mathbf{i}} \frac{2\pi\hbar^2}{m} b \delta(\mathbf{x} - \mathbf{R}_{\mathbf{i}}) + \sum_{\mathbf{i}} \left(\frac{\mathbf{P}_{\mathbf{i}}}{2M} \right)^2 + \sum_{\mathbf{i}\mathbf{i}'} \frac{1}{2} \tilde{\mathbf{U}}_{\mathbf{i}} M \tilde{\mathbf{U}}_{\mathbf{i}'}, \quad (1)$$

We have written the crystal potential due to the motion of ions in the harmonic approximation. We have expressed the neutron potential energy in Fermi-pseudopotential form.¹⁰ Also, we have assumed for simplicity that nuclei with identical scattering amplitude b and mass M occupy the sites of a Bravais lattice. If we write the lattice coordinates as $\mathbf{R}_{\mathbf{i}} = \mathbf{l} + \tilde{\mathbf{u}}_{\mathbf{i}}$ and make the Taylor expansion of $\delta(\mathbf{x} - \mathbf{R}_{\mathbf{i}})$ for small $\tilde{\mathbf{u}}_{\mathbf{i}}$, the Hamiltonian becomes

$$H = \frac{1}{2m} \left(\frac{\hbar}{i} \frac{\partial}{\partial \mathbf{x}} \right)^2 + \sum_{\mathbf{i}} \frac{2\pi\hbar^2}{m} b \delta(\mathbf{x} - \mathbf{l}) + \sum_{\mathbf{q}} a_{\mathbf{q}}^{\dagger} a_{\mathbf{q}} \hbar\omega(\mathbf{q}) + \frac{2\pi\hbar^2}{m} \frac{b}{v_0} \sum_{\mathbf{k}} e^{-i\mathbf{k} \cdot \mathbf{x}} \sum_{\mathbf{q}} \left(\frac{\hbar}{2MN\omega(\mathbf{q})} \right)^{1/2} \times [i\tilde{\boldsymbol{\epsilon}}_{\mathbf{q}} \cdot (\mathbf{q} - \mathbf{g}) e^{i\mathbf{q} \cdot \mathbf{x}} a_{\mathbf{q}} + -i\tilde{\boldsymbol{\epsilon}}_{\mathbf{q}}^* \cdot (\mathbf{q} + \mathbf{g}) e^{-i\mathbf{q} \cdot \mathbf{x}} a_{\mathbf{q}}^{\dagger}]. \quad (2)$$

In formulating a dynamical theory, it is advantageous to express the Hamiltonian in spatial coordinates of the neutron. In the above, we have used a rigid-ion approximation¹¹ in writing the interaction of the neutron with the nuclei of the lattice. This approximation is justified by the extremely short-range nature of the neutron-nucleon interaction.

Since we are interested in the inelastic transition rate, we use time-dependent perturbation theory. We take the unperturbed Hamiltonian

$$H_0 = -\frac{\hbar^2}{2m} \frac{\partial^2}{\partial \mathbf{x}^2} + \sum_{\mathbf{i}} \frac{2\pi\hbar^2}{m} b \delta(\mathbf{x} - \mathbf{l}) + \sum_{\mathbf{q}} \hbar\omega(\mathbf{q}) a_{\mathbf{q}}^{\dagger} a_{\mathbf{q}} = H_{0n} + H_{0c} \quad (3)$$

and its eigenstates as bases for expansion of the wave function $\Psi(\mathbf{x}, t)$ of the total Hamiltonian, satisfying

$$(H_0 + H_1)\Psi(\mathbf{x}, t) = i\hbar \frac{\partial}{\partial t} \Psi(\mathbf{x}, t). \quad (4)$$

The above division of the total Hamiltonian is different from the usual one. Usually the unperturbed part includes only the kinetic-energy term of the neutron. In our case, since we already know the exact solution of elastic scattering from the static lattice (Paper I), it is advantageous to make this type of division along the lines of the distort-

ed-wave Born approximation.

The eigenstates of H_0 are given by $\phi_{\mathbf{k}i}(\mathbf{x})\{|N_{\mathbf{q}}\rangle\}$, where $\phi_{\mathbf{k}i}(\mathbf{x})$ is a Bloch wave function (eigenfunction of H_{0n}) and $\{|N_{\mathbf{q}}\rangle\}$ is a phonon occupation distribution. The eigenstates $\phi_{\mathbf{k}i}(\mathbf{x})$, however, do not provide the most suitable basis for the expansion of $\Psi(\mathbf{x}, t)$, because they do not explicitly contain boundary conditions at $z=0$ and $z=D$. Therefore, we consider two orthonormal sets that satisfy boundary conditions and are defined in the following manner:

$$\Psi_{k_0g}(\mathbf{x}) = \sum_{\mathbf{i}} \alpha_{i_g} \phi_{\mathbf{k}i}(\mathbf{x}), \quad (5)$$

$$\sum_{\mathbf{i}} \alpha_{i_g} U_{g'}^i = \delta_{g'g},$$

$$\phi_{\mathbf{k}i}(\mathbf{x}) = \frac{1}{V^{1/2}} \sum_{\mathbf{k}} U_{\mathbf{k}}^i e^{i(\mathbf{k}i + \mathbf{k}) \cdot \mathbf{x}}, \quad (6)$$

and

$$\Psi^{k_0g}(\mathbf{x}) = \sum_{\mathbf{i}} \alpha_{\mathbf{i}}^g \phi_{\mathbf{k}i}(\mathbf{x}), \quad (7)$$

$$\sum_{\mathbf{i}} \alpha_{\mathbf{i}}^g U_{g'}^i e^{i\gamma_{g'}^i D} = \delta_{g'g} e^{i\Gamma_g D}.$$

Parameters γ_g and Γ_g are explained in Paper I. The orthonormality of wave functions Ψ_{k_0g} and Ψ^{k_0g} can easily be proved by the procedure outlined in the Appendix of Ref. 8 (the proof has been detailed in Ref. 16). The subscript k_0 refers to the wave vector, in vacuum, of the neutron for which the Bloch waves $\phi_{\mathbf{k}i}$ are solutions of H_0 . Thus Ψ_{k_0g} represents the wave function (in the crystal) which, at the boundary $z=D$, matches the wave function (plane wave) of the neutron scattered in the direction $\mathbf{k}_0 + \mathbf{g}$, and satisfies the boundary condition. In elastic diffraction theory (Paper I), it is the amplitude of Ψ_{k_0g} that determines the intensity of the diffracted wave in the \mathbf{g} direction. In the inelastic case, however, the interaction Hamiltonian H_I causes transitions between different states represented by Ψ_{k_0g} and the initial state, chosen appropriately from the set Ψ_{k_0g} .

We write the wave function $\Psi(\mathbf{x}, t)$ as

$$\Psi(\mathbf{x}, t) = \sum_{k_0, N, g} C_{k_0, N, g}(t) \Psi_{k_0g}(\mathbf{x}) \{|N_{\mathbf{q}}\rangle\} \times \exp\left[-\left(\frac{i}{\hbar}\right)(E_{k_0} + E_N)t\right] + \sum_{k_0', g', N_{\mathbf{q}}' \neq N_{\mathbf{q}}} C_{N_{\mathbf{q}}'}^{k_0'g'} \Psi^{k_0'g'}(\mathbf{x}) \{|N_{\mathbf{q}}'\rangle\} \times \exp\left[-\left(\frac{i}{\hbar}\right)(E_{k_0'} + E_{N'})t\right], \quad (8)$$

$$E_N = \sum_{\mathbf{q}} \hbar N_{\mathbf{q}} \omega(\mathbf{q}).$$

The initial conditions on the expansion coefficients C are

$$C_{k_0, N_q}(t=0) = 1, \quad C_{N'_q, k_0}(t=0) = 0.$$

From first-order perturbation theory,

$$C_{N'_q, k_0}(t) = \langle N'_q \Psi_{k_0, g'} | H_I | N_q \Psi_{k_0, g} \rangle \frac{e^{-i(\hbar/\Delta E)t} - 1}{\Delta E}, \quad (9)$$

where

$$\Delta E = E_{k_0} + E_N - E_{k_0} - E_{N'},$$

$$\begin{aligned} & \langle N'_q \Psi_{k_0, g'} | H_I | N_q \Psi_{k_0, g} \rangle \\ &= \sum_{q, G} V_{qG} \int_V \Psi_{k_0, g'}^*(\vec{x}) e^{i(\vec{q}-\vec{G}) \cdot \vec{x}} \Psi_{k_0, g}(\vec{x}) d^3x \\ &+ \sum_{q, G} V_{qG}^* \int_V \Psi_{k_0, g}^*(\vec{x}) e^{-i(\vec{q}+\vec{G}) \cdot \vec{x}} \Psi_{k_0, g'}(\vec{x}) d^3x. \end{aligned} \quad (10)$$

Here V is the volume of the crystal, and V_{qG} is defined by Eq. (2). In the following discussion we limit ourselves to the measurement of the energy-loss inelastic peak corresponding to the creation of a phonon in the crystal. The energy-gain peak can be considered on completely analogous lines. To proceed in computing the transition matrix element $\langle N' \Psi' | H_I | N \Psi \rangle$, we take our measurement geometry as defined in Fig. 1. We assume that the amplitude of the incoming wave is unity and therefore, in the incident-wave orthogonal set $\Psi_{k_0, g}$, the only nonzero member is $\Psi_{k_0, 0}$. For the incident side, the choice of zero for the reciprocal space is a natural one; for the exit side, however,

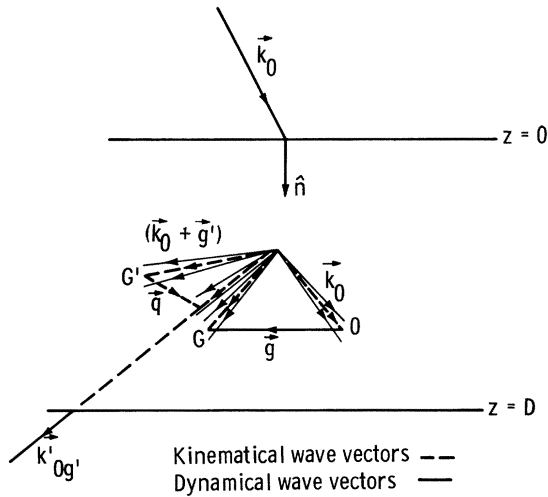


FIG. 1. Schematic illustration of wave vectors for kinematical and dynamical theory in the inelastic cross-section measurement for a phonon wave vector \vec{q} . Dynamical effects are due to only two points, O and G , on the Ewald sphere.

the choice is arbitrary. We take $\vec{k}'_{0g'}$ to be the principal exit-side wave vector; others are defined from \vec{g}' as the reference. The vector \vec{g}' is the reciprocal-lattice point at which energy-momentum conservation conditions are satisfied for the phonon wave vector \vec{q} under investigation.

Thus, for example, if the inelastically scattered wave $(\vec{k}_0 - \vec{g}' - \vec{q})$ is Bragg scattered by lattice planes \vec{h}' , then in the expansion (6) $\vec{g} = \vec{g}'$ and the plane-wave amplitudes $U_{g'}^i$ and $U_{g'+h'}^i$ are the only important amplitudes in the Bloch wave ϕ_{k_i} representing inelastic scattering at \vec{g}' .

With the above considerations from Eq. (5), (7), and (10),

$$\begin{aligned} \langle H_I \rangle &= -\frac{i}{D} \sum_{hh'} V_{g'+h', -h}^*(\vec{q}) \sum_{ii'} \alpha_{i0} U_h^i \alpha'_{i'h'} U_{g'+h'}^{*i'} \\ &\times \frac{(2\pi)^2}{S} \delta(\vec{k}_0 + \vec{q} - \vec{k}'_{0g'})_t \\ &\times \frac{\exp(i\Delta k_q^{ii'} D) - 1}{i\Delta k_q^{ii'} D}. \end{aligned} \quad (11)$$

Here S is the surface area of the crystal, which we have assumed to be so large that the limits in the integrals over the surface coordinates in the matrix element are essentially $-\infty$ and $+\infty$. Also, $\Delta k_q^{ii'} = (\gamma^i - q_n - \gamma'^{i'})$ in the notation of Ref. 1, and q_n is the normal component of the phonon wave vector \vec{q} . The subscript t in the δ -function argument denotes the tangential component of the vector argument. From Eq. (11) the remarkable distinguishing features of dynamical theory should be obvious: (a) We no longer have the conservation of linear momentum in the direction normal to the crystal surface; and (b) in the inelastic amplitude, *all* the plane-wave components, U_h^i and $U_{g'+h'}^{i'}$, contribute with their respective amplitudes α_i and $\alpha'_{i'h'}$. It is the last factor in Eq. (11) that will give the thickness- or wavelength-dependent structure in the inelastic peak. If the crystal were thick ($\Delta k_q^{ii'} D \gg 1$), we would get a δ function for the conservation of the normal component of the momentum.

Equation (11), together with (5) and (7), determines the matrix element of interaction. Therefore, the time-dependent amplitudes of various states in the expansion of wave function $\Psi(\vec{x}, t)$ in Eq. (8) become known.

II. INELASTIC PEAK INTENSITY

The rate of transition to a group of states between the neutron energy $E_{k_0, g'}$ and $E_{k_0, g'} + \Delta E$ is given by

$$P = \frac{1}{\hbar^2} \int_{\Delta E} |\langle H_I \rangle|^2 \delta \left(\frac{E_{k_0} - E_{k'_{0g'}} - \hbar \omega(q)}{2\hbar} \right) \times \rho_n(E_{k'_{0g'}}) dE_{k'_{0g'}}. \quad (12)$$

Here $\rho_n(E_{k'_{0g'}})$ is the density of neutron states at the wave vector $\vec{k}'_{0g'}$. We shall assume that our inelastic peak is very sharp in the energy variable, and that we have set our detection equipment in such a way that the energy-conservation condition is satisfied for a given \vec{q} . In our choice of \vec{q} we are guided by the kinematical approximation of our dynamical theory. The transition rate is then given by

$$P = \frac{2\pi}{\hbar} |\langle H_I \rangle|^2 \rho_n(E_{k'_{0g'}}) = \frac{2\pi}{\hbar} \left| \sum_{q_n} \sum_{hh'ii'} V_{g'+h',-h}^* (\vec{q}) \alpha_{i_0} U_h \alpha_{i',g'} U_{g'+h'}^{i*} \times \frac{1}{iD} \frac{\exp(i\Delta k_q^{ii'} D) - 1}{\Delta k_q^{ii'}} \right|^2 \rho_n. \quad (13)$$

In this equation the summation is over those values of q_n that satisfy the energy-conservation condition and the conservation of the tangential component of the momentum. Figure 2 explains the q_n s that are relevant at energy $E_{k'_{0g'}}$. The loci of various wave vectors have been denoted by their energy. The circles in Fig 2 are in fact projec-

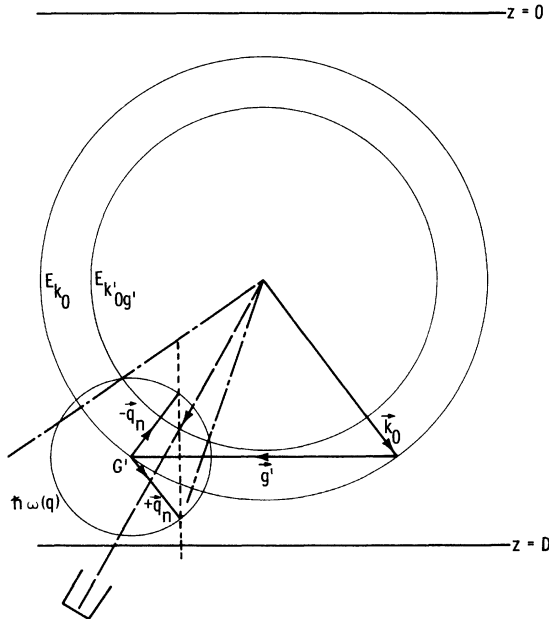


FIG. 2. Geometrical construction for determining the phonon wave vectors $+q_n$ and $-q_n$ that contribute to the inelastic dynamic effects at a given angular setting of the detector.

tions of the spheres on the plane of observation, i.e., the scattering plane. The only phonon wave vectors that satisfy the conservation of the tangential component of the momentum as well as the conservation of energy are $+q_n$ and $-q_n$ in Fig. 2. All other phonon wave vectors give a nonzero out-of-scattering-plane component to the exit-region neutron wave vector. The contribution of q_n enters in the exponential factor in Eq. (14). The values of γ^i and $\gamma_{g'}^i$ differ by very small amounts (δ_i and $\delta'_{i'}$) from their kinematical counterparts Γ_0 and $\Gamma'_{0g'}$. Therefore, unless the q_n values (determined unambiguously by the setting of the detector) are close to $\Gamma_0 - \Gamma'_{0g'}$ (i.e., almost satisfying the conservation of the normal component of momentum), the transition rate would be essentially zero, because of the exponential factor and the associated denominator. In other words, violation of the conservation of the normal components of the wave vectors is tolerated only to the order of splitting of the neutron wave vectors caused by elastic interaction with the static lattice. In particular, if the detector is oriented to receive the sharp peak of a certain phonon \vec{Q} , and there is no Bragg scattering of the wave vector $k'_{0g'}$ from any set of lattice planes, then $\exp(i\Delta k_q^{ii'} D)$ becomes simply $e^{i\delta_i D}$, where $\delta_i = \gamma_i - \Gamma_0$. The angle of orientation of the detector is determined by kinematical considerations; in Fig. 2, for the given energy $E_{k'_{0g'}}$, the proper direction is shown by a dash-dot line. The exponential factor is the same as in the dynamical theory for elastic diffraction (Paper I).

From the above considerations, the intensity of the sharp inelastic peak, when the narrow energy window of the detector receives all the peak, is given by

$$I_{q'} = \frac{2\pi}{\hbar} \left| \sum_{ii'} B_{ii'}^{g'} \frac{\exp(i\Delta k_q^{ii'} D) - 1}{\Delta k_q^{ii'} D} \right|^2, \quad (14)$$

$$B_{ii'}^{g'} = \sum_{hh'} V_{g'+h',-h}^* (\vec{q}) \alpha_{i_0} U_h^i \alpha_{i',g'} U_{g'+h'}^{i*}, \quad (15)$$

$$\Delta k_q^{ii'} = \gamma_i - \gamma_{g'}^{i'} - q_n = \delta_i - \delta'_{i'}.$$

Equation (14), together with Eq. (15), makes up the most general expression for the intensity of the inelastic peak. It leads to a complicated structure in the inelastic peak if the U factors—i.e., amplitudes of the plane-wave components in the Bloch waves—are non-negligible for more than two reciprocal-lattice vectors in the incident side as well as the exit side. For the two-beam approximation, various factors of Eq. (15) are easily determined; they are tabulated in the Appendix.

III. INELASTIC PENDELLÖSUNG

In the following we specialize the general expression (14) to a particular situation that shows

some interesting features.

There are two configurations of experimental geometry in which the thickness dependence of the peak intensity takes a comparatively simple form: (a) The incident wave vector satisfies the Bragg condition only for the set of planes denoted by H ; the inelastically scattered wave vector $k'_{0g'}$ does not satisfy the Bragg condition for any plane. (b) The incident wave vector does not satisfy the Bragg condition, but the scattered wave vector satisfies the Bragg condition for the reciprocal vector H' .

The two cases are completely analogous. We discuss case (a) first. We further simplify matters by assuming that the crystal is oriented so that the reciprocal-lattice vector H in question is parallel to the incident-side boundary $z=0$, and we define the scattering plane by $y=0$. Then the inelastic intensity around the reciprocal-lattice vector \vec{g}' is given by

$$I_{g'} = \frac{2\pi}{\hbar} \left| V_{g'}^*(\vec{q}) \left(\alpha_{10} U_0^1 \frac{e^{i\delta_1 D} - 1}{i\delta_1 D} + \alpha_{20} U_0^2 \frac{e^{i\delta_2 D} - 1}{i\delta_2 D} \right) + V_{g'-H}^*(\vec{q}) \left(\alpha_{10} U_H^1 \frac{e^{i\delta_1 D} - 1}{i\delta_1 D} + \alpha_{20} U_H^2 \frac{e^{i\delta_2 D} - 1}{i\delta_2 D} \right) \right|^2, \quad (16)$$

where

$$\delta_{1,2} = \gamma^{1,2} - \Gamma_0 = -\frac{V_0}{2\Gamma_0} \mp \frac{V_H}{2\Gamma_0}.$$

If we write $V_H = (V_{-H})^* = |V_H| e^{i\theta_H}$, then $w_1 = -e^{-i\theta_H}$ and $w_2 = +e^{-i\theta_H}$ (see Appendix). The intensity is then given by

$$I_{g'} = \frac{2\pi}{\hbar} \frac{1}{4} \left| V_{g'}^*(\vec{q}) \left(e^{i(\delta_1 D/2)} \frac{\sin(\delta_1 D/2)}{\delta_1 D/2} + e^{i(\delta_2 D/2)} \frac{\sin(\delta_2 D/2)}{\delta_2 D/2} \right) + V_{g'-H}^*(\vec{q}) e^{i\theta_H} \left(-e^{i(\delta_1 D/2)} \frac{\sin(\delta_1 D/2)}{\delta_1 D/2} + e^{i(\delta_2 D/2)} \frac{\sin(\delta_2 D/2)}{\delta_2 D/2} \right) \right|^2. \quad (17)$$

$$I_{g'} = \frac{2\pi}{\hbar} |V_{g'}^*(\vec{q})|^2 \times \frac{1}{4} \left\{ |1-p|^2 \left(\frac{\sin(\delta_1 D/2)}{\delta_1 D/2} \right)^2 + |1+p|^2 + 2 \frac{\sin(\delta_1 D/2)}{\delta_1 D/2} \left[(1-|p|)^2 \cos\left(\frac{\delta_1 D}{2}\right) + 2\text{Im}p \sin\left(\frac{\delta_1 D}{2}\right) \right] \right\}. \quad (20)$$

Fortunately this restriction, $V_0 = |V_H|$, can be realized in many cases. For a diamond-type structure (e.g., Si and Ge), the requirement translates into hkl unmixed and $h+k+l=4n$, where n

Equation (17) shows clearly the physical effect of dynamical diffraction on inelastic scattering. The inelastic amplitude consists of four terms, each of which represents the role of one of the four plane-wave components (with their proper amplitudes) that make up the two Bloch waves (\vec{k}^1 and \vec{k}^2) of the elastic diffraction from the set of lattice planes H . There are two distinct *Pendellösung* periods, corresponding to δ_1 and δ_2 . This situation is different from the *Pendellösung* in the elastic theory. There, the period is proportional to $\delta_1 - \delta_2 = \Delta$ and depends only on V_H . Here, the mean lattice potential V_0 of the neutron-lattice interaction is also important. The neutron-phonon interaction terms $V(\vec{q})$ that enter into Eq. (17) are consistent with this physical picture of inelastic scattering.

We can rewrite Eq. (17) as follows:

$$I_{g'} = \frac{2\pi}{\hbar} |V_{g'}^*(\vec{q})|^2 \times \frac{1}{4} \left\{ |1-p|^2 \frac{\sin^2(\delta_1 D/2)}{(\delta_1 D/2)^2} + |1+p|^2 \frac{\sin^2(\delta_2 D/2)}{(\delta_2 D/2)^2} + 2 \frac{\sin(\delta_1 D/2) \sin(\delta_2 D/2)}{(\delta_1 D/2)(\delta_2 D/2)} + \left[(1-|p|)^2 \cos\left(\frac{\Delta D}{2}\right) + 2\text{Im}p \sin\left(\frac{\Delta D}{2}\right) \right] \right\}, \quad (18)$$

$$p \equiv \frac{V_{g'-H}^*(\vec{q})}{V_{g'}^*(\vec{q})} e^{i\theta_H} = \left| \frac{\vec{\epsilon}_q \cdot (\vec{q} + \vec{g}' - \vec{H})}{\vec{\epsilon}_q \cdot (\vec{q} + \vec{g}')} \right| e^{i\theta_H}, \quad (19)$$

$$\Delta = \delta_1 - \delta_2 = |V_H|/\Gamma_0.$$

Equation (18) shows that the structure in the inelastic peak, which is dependent on thickness or incident wavelength, is much more complicated than that in the elastic peak. However, there are certain situations in which some simplifications occur. If $V_0 = |V_H|$, then $\delta_2 = 0$ and there is only one *Pendellösung* period. The intensity is then

is an integer. For such a structure, (220) is the lowest-order peak that would satisfy the above restriction.

In Eq. (20), if $p=0$ the intensity is given by

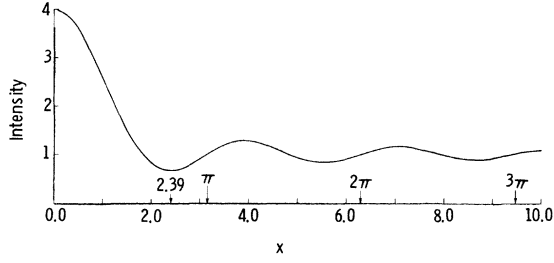


FIG. 3. Intensity variation of the one-phonon peak. Here $x = D\lambda/48 \cos\theta_B$ for Si(220); D is in μ ; λ is the incident neutron wavelength, in \AA ; and θ_B is the Bragg angle.

$$I_{g'} = \frac{2\pi}{h} |V_g^*(\vec{q})|^2 \frac{1}{4} \left[\left(\frac{\sin x}{x} \right)^2 + 1 + 2 \left(\frac{\sin x}{x} \right) \cos x \right], \quad (21)$$

where $x \equiv \frac{1}{2} \delta_1 D$. The function within the brackets has been plotted in Fig. 3. Although the intensity variation with respect to thickness is *somewhat* similar to the *Pendellösung* phenomenon, the first extinction distance is given by $\delta_1 D/2 = 2.39$, compared to 3.14 (π) for the elastic *Pendellösung* extinction distance. The function, however, assumes the value 1 at $x = n\pi$, the zeroes of $(\sin x/x)^2$.

For a diamond-type lattice, the realization of $p=0$ is demonstrated in Fig. 4. The figure, though schematic, has been drawn approximately to scale. The figure indicates the projection of the reciprocal lattice of Si on the $(1\bar{1}0)$ plane. $\vec{H} = (2, 2, 0)$ and $\vec{g} = (\bar{1}, \bar{1}, 1)$. In order to get $p=0$, we find \vec{q} such that \vec{e}_q , the polarization vector, is perpendicular to the scattering vector $\vec{q} + \vec{g}' - \vec{H}$. This can be done done, for example, by drawing the ‘‘scattering surface’’¹² around $(\bar{1}\bar{1}1)$ for a suitable incident wave vector and then finding the intersection of this surface with a sphere drawn on the vector $\vec{g}' - \vec{H}$. The point of intersection gives the desired \vec{q} for longitudinal phonons. For illustration, we

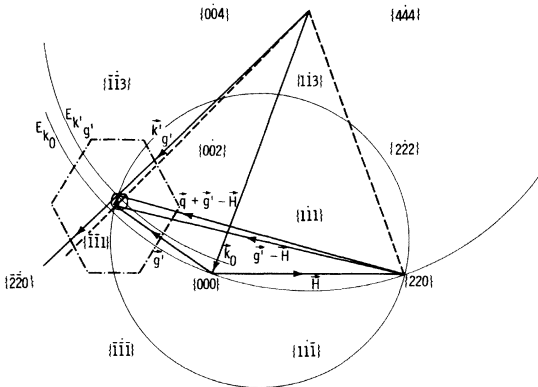


FIG. 4. Projection of reciprocal lattice of Si on $(1\bar{1}0)$ plane. See text for details.

have taken the approximate dispersion curves of LA phonons for Si from Ref. 13 and shown the trace of the scattering surface on the $(1\bar{1}0)$ plane. Also shown is the first Brillouin zone. For the TA phonons, the geometrical construction would require determination of the intersection of the scattering surface trace with the vector $\vec{g}' - \vec{H}$ itself.

From the above considerations, the following experiment can be suggested for the observation of the *Pendellösung* phenomenon in the inelastic peak. Si or Ge crystals in the form of thin parallel plates of different thicknesses should be cut for the observation of the (220) elastic peak in the symmetrical Laue configuration. The requirement can be satisfied with a crystal grown in the $[100]$ direction and sliced along the length of the axis. The incident wavelength should be so chosen that no other elastic peak is excited. In order to approximate our theoretical formulation as closely as possible, the energy-momentum window of the detector must be narrowly centered around the maximum of the inelastic peak of the phonon, determined from a construction like that in Fig. 4. The same experimental configuration would also give the excitation distance of the elastic (220) peak; therefore the two extinction distances can be compared easily. For the incident-neutron wavelength used in our example, 1.25 \AA , the extinction distance is 19 μm ; for the elastic peak it is 25 μm .

In the above we have discussed the energy-loss peak. The treatment of the energy-gain peak is completely analogous, and gives the same extinction thickness if the restrictions described in the preceding paragraphs are met; the proper \vec{q} at which the *Pendellösung* would be observed, however, will be different. Similar treatment applies to case (b), in which the inelastically scattered beam satisfies the Bragg condition for \vec{H}' planes.

IV. CONCLUSION AND DISCUSSION

We have presented a simple picture of the first-order effects of the dynamical theory of diffraction on one-phonon inelastic scattering. The amplitude of this scattering is the coherent sum of the amplitudes due to all the plane-wave components that form the exact wave function of the neutron in the static lattice. This wave function depends on the incident wavelength and other parameters of the experimental geometry. The amplitude of the inelastically scattered wave is further subject to dynamical effects of the static lattice under favorable experimental situations. We have taken into account the scattering of the neutron from the static lattice to all orders by suitable par-

tioning the Hamiltonian of the neutron-lattice system, but we have treated the inelastic scattering to the first order in the neutron-phonon interaction. This approximation can be justified on the ground that neutron-phonon interaction is of the order of $1/N^{1/2}$ times the interaction of neutrons with the static lattice. Thus our approximation becomes quite good if the multiphonon contribution to the inelastic peak is negligibly small.

The formulation we have given shows the advantage of the distorted-wave Born approximation (DWBA) over the simple Born approximation. The latter considers all of the interaction as a perturbation over the kinetic energy. Therefore, if one uses the field-theoretic language to describe the inelastic scattering, and starts with Green's function for the unperturbed Hamiltonian as due only to the kinetic energy of the neutron, one has to sum an infinite order of diagrams to arrive at the result that the Bloch wave function completely describes the interaction in the static lattice. In DWBA we start with the Bloch wave function and the associated Hamiltonian as unperturbed quantities, and avoid the summation of diagrams.¹⁴ In our case, we believe, this is the central advantage of DWBA over the usual perturbation theory.

The *Pendellösung* phenomenon in the inelastic one-phonon peak, which we suggested in Sec. III, cannot be observed in conventional x-ray and electron diffraction arrangements. This is so either because the energy resolution of the detection equipment is not fine enough to measure accurately the one-phonon peak in the inelastically scattered beam (x rays), or because the magnitude of the incident wave vector is such that the

two-beam diffraction conditions cannot be satisfied exclusively for high-energy electron diffraction. For low-energy electron diffraction, they can be satisfied exclusively, but transmission-type experiments are ruled out by a very low depth of penetration of electrons. The experimental configuration that Shull¹⁵ used for his elastic *Pendellösung* could perhaps be used to investigate the feasibility of the experiment suggested here.

ACKNOWLEDGMENTS

I am grateful to Professor M. Blume, under whose guidance this work was done. I am thankful to my colleagues I. M. Held, J. M. Andrade, and K. Sarkaria for helpful discussions.

APPENDIX

Factors in the transition matrix element corresponding to the incident side:

$$\alpha_{1,0}U_0^1 = \frac{w_1}{(1+|w_1|^2)^{1/2}} \frac{w_1}{(1+|w_1|^2)^{1/2}} = \frac{|w_1|^2}{1+|w_1|^2},$$

$$\alpha_{2,0}U_0^2 = \frac{w_2^*}{(1+|w_2|^2)^{1/2}} \frac{w_2}{(1+|w_2|^2)^{1/2}} = \frac{w_2^2}{1+|w_2|^2},$$

$$\alpha_{1,0}U_g^1 = \frac{w_1^*}{(1+|w_1|^2)^{1/2}} \frac{1}{(1+|w_1|^2)^{1/2}} = \frac{w_1^*}{1+|w_1|^2},$$

$$\alpha_{2,0}U_g^2 = \frac{w_2^*}{(1+|w_2|^2)^{1/2}} \frac{1}{(1+|w_2|^2)^{1/2}} = \frac{w_2^*}{1+|w_2|^2}.$$

For the symmetrical Laue configuration at exactly Bragg incidence,

$$w_{1,2} = \frac{V_{-g}}{2\Gamma_0\delta_{1,2} + V_0} = -\frac{V_{-g}}{\pm|V_g|} \equiv \mp e^{-i\theta_g}.$$

We have assumed real scattering amplitudes for the nucleons of the lattice.

*Based in part on the Ph.D. thesis submitted at State University of New York, Stony Brook, New York, 1974.

†Present address: Universidade de Aveiro, Aveiro, Portugal.

¹Sushil Kumar Mendiratta and M. Blume, Phys. Rev. B **14**, 144 (1976).

²H. Yoshioka, J. Phys. Soc. Jpn. **12**, 618 (1957).

³Y. Kainuma, Acta Crystallogr. **8**, 247 (1955).

⁴M. Ichikawa and Y. H. Ohtsuki, J. Phys. Soc. Jpn. **27**, 953 (1969).

⁵M. P. Seah, Surf. Sci. **17**, 161 (1969); **17**, 132 (1969); J. A. Strozier and R. O. Jones, Phys. Rev. B **3**, 3228 (1971).

⁶M. J. Whelan, in *Modern Diffraction and Imaging Techniques in Materials Science*, edited by S. Amelinx et al. (North-Holland, Amsterdam, 1970).

⁷A. Howie, Proc. R. Soc. A **271**, 268 (1962).

⁸F. Fujimoto and Y. Kainuma, J. Phys. Soc. Jpn. **18**, 1792 (1963).

⁹S. Takagi, J. Phys. Soc. Jpn. **13**, 278 (1958).

¹⁰W. Marshall and S. W. Lovesey, *Theory of Thermal Neutron Scattering* (Oxford U.P., Oxford, England, 1971), p. 8.

¹¹For example, R. P. Feynman, *Statistical Mechanics* (Benjamin, New York, 1972), p. 188.

¹²G. Placzek and L. van Hove, Phys. Rev. **93**, 1207 (1954).

¹³B. N. Brockhouse, in *Phonons and Phonon Interactions*, edited by T. Bak (Benjamin, New York, 1964), p. 256.

¹⁴C. B. Duke and U. Landman, Phys. Rev. B **6**, 2956 (1972), and references cited therein.

¹⁵C. G. Shull, Phys. Rev. Lett. **21**, 1585 (1968).